AFRL-ML-WP-TM-2004-4141

NONDESTRUCTIVE EVALUATION (NDE) TECHNOLOGY INITIATIVES PROGRAM (NTIP)

Delivery Order 0029: Advanced Thermosonic Methods (SONIC IR)

By:
Donna Mayton and Eric Lindgren

SAIC/Ultra Image International
Two Shaw's Cove
Suite 101
New London, CT 06320

For:

Universal Technology Corporation
1270 North Fairfield Road
Dayton, OH 45432-2600

JULY 2003

Final Report for 01 March 2002 – 01 May 2003

STINFO FINAL REPORT

MATERIALS AND MANUFACTURING DIRECTORATE
AIR FORCE RESEARCH LABORATORY
AIR FORCE MATERIEL COMMAND
WRIGHT-PATTERSON AIR FORCE BASE, OH 45433-7750

NOTICE

WHEN GOVERNMENT DRAWINGS, SPECIFICATIONS, OR OTHER DATA ARE USED FOR ANY PURPOSE OTHER THAN IN CONNECTION WITH A DEFINITELY GOVERNMENT-RELATED PROCUREMENT, THE UNITED STATES GOVERNMENT INCURS NO RESPONSIBILITY OR ANY OBLIGATION WHATSOEVER. THE FACT THAT THE GOVERNMENT MAY HAVE FORMULATED OR IN ANY WAY SUPPLIED THE SAID DRAWINGS, SPECIFICATIONS, OR OTHER DATA, IS NOT TO BE REGARDED BY IMPLICATION OR OTHERWISE IN ANY MANNER CONSTRUED, AS LICENSING THE HOLDER OR ANY OTHER PERSON OR CORPORATION, OR AS CONVEYING ANY RIGHTS OR PERMISSION TO MANUFACTURE, USE, OR SELL ANY PATENTED INVENTION THAT MAY IN ANY WAY BE RELATED THERETO.

THIS REPORT HAS BEEN REVIEWED BY THE OFFICE OF PUBLIC AFFAIRS (ASC/PA) AND IS RELEASABLE TO THE NATIONAL TECHNICAL INFORMATION SERVICE (NTIS). AT NTIS, IT WILL BE AVAILABLE TO THE GENERAL PUBLIC, INCLUDING FOREIGN NATIONS.

THIS TECHNICAL REPORT HAS BEEN REVIEWED AND IS APPROVED FOR PUBLICATION.

/s/
JUAN CALZADA, Project Engineer
Nondestructive Evaluation Branch
Metals, Ceramics & NDE Division

/s/
JAMES C. MALAS, Chief
Nondestructive Evaluation Branch
Metals, Ceramics & NDE Division

/s/
GERALD J. PETRAK, Assistant Chief
Metals, Ceramics & NDE Division
Materials & Manufacturing Directorate

IF YOUR ADDRESS HAS CHANGED, IF YOU WISH TO BE REMOVED FROM OUR MAILING LIST, OR IF THE ADDRESSEE IS NO LONGER EMPLOYED BY YOUR ORGANIZATION, PLEASE NOTIFY, AFRL/MLLP, WRIGHT-PATTERSON AFB OH 45433-7817 TO HELP US MAINTAIN A CURRENT MAILING LIST.

COPIES OF THIS REPORT SHOULD NOT BE RETURNED UNLESS RETURN IS REQUIRED BY SECURITY CONSIDERATIONS, CONTRACTUAL OBLIGATIONS, OR NOTICE ON A SPECIFIC DOCUMENT.

REPORT DOCUMENTATION PAGE

Form Approved
OMB No. 0704-0188

1. REPORT DATE *(DD-MM-YY)*	2. REPORT TYPE	3. DATES COVERED *(From - To)*
July 2003	Final	03/01/2002 – 05/01/2003

4. TITLE AND SUBTITLE
NONDESTRUCTIVE EVALUATION (NDE) TECHNOLOGY INITIATIVES PROGRAM (NTIP)
Delivery Order 0029: Advanced Thermosonic Methods (SONIC IR)

5a. CONTRACT NUMBER
F33615-97-D-5271-0029

5b. GRANT NUMBER

5c. PROGRAM ELEMENT NUMBER
62102F

6. AUTHOR(S)
Donna Mayton and Eric Lindgren

5d. PROJECT NUMBER
4349

5e. TASK NUMBER
40

5f. WORK UNIT NUMBER
01

7. PERFORMING ORGANIZATION NAME(S) AND ADDRESS(ES)

By:	For:
SAIC/Ultra Image International Two Shaw's Cove Suite 101 New London, CT 06320	Universal Technology Corporation 1270 North Fairfield Road Dayton, OH 45432-2600

8. PERFORMING ORGANIZATION REPORT NUMBER

9. SPONSORING/MONITORING AGENCY NAME(S) AND ADDRESS(ES)
Materials and Manufacturing Directorate
Air Force Research Laboratory
Air Force Materiel Command
Wright-Patterson AFB, OH 45433-7750

10. SPONSORING/MONITORING AGENCY ACRONYM(S)
AFRL/MLLP

11. SPONSORING/MONITORING AGENCY REPORT NUMBER(S)
AFRL-ML-WP-TM-2004-4141

12. DISTRIBUTION/AVAILABILITY STATEMENT
Approved for public release; release is unlimited.

13. SUPPLEMENTARY NOTES
Report contains color.

14. ABSTRACT

The overall objective of this program was to demonstrate that the Sonic Infrared (IR) inspection technique can be used reliably to detect a fatigue crack located at the anti-rotation feature on the F100 first stage turbine disk. As the physics of the mechanical energy to thermal energy conversion for this technique is not well understood at this time, an empirical approach was used to develop the system parameters that will enable a reproducible inspection technique to be developed. This Delivery Order covered a literature and subject matter expert search, development of a Design of Experiments (DoE) test plan, production of a test fixture, and preliminary interface and fixturing materials testing. Fixturing and coupling were identified as key parameters for reliability. Testing was continued on a follow-on program.

15. SUBJECT TERMS
Thermosonics, Sonic IR, Vibrothermography

16. SECURITY CLASSIFICATION OF:			17. LIMITATION OF ABSTRACT:	18. NUMBER OF PAGES	19a. NAME OF RESPONSIBLE PERSON (Monitor)
a. REPORT	b. ABSTRACT	c. THIS PAGE			Juan Calzada
Unclassified	Unclassified	Unclassified	SAR	32	19b. TELEPHONE NUMBER *(Include Area Code)* (937) 255-1605

Standard Form 298 (Rev. 8-98)
Prescribed by ANSI Std. Z39-18

TABLE OF CONTENTS

LIST OF FIGURES AND TABLES

Figures

Tables

Advanced Thermosonic Methods (Sonic IR)

Introduction

The Materials and Manufacturing Directorate of the Air Force Research Laboratory (AFRL) has initiated a Sonic IR program with SAIC Ultra Image International through Universal Technology Corporation. The AFRL point of contact for this program is Tom Moran from the Nondestructive Evaluation Branch. The program will support the Engine Structural Integrity and Engine Rotor Life Extension Programs of the Air Force. The program includes participation by Wayne State University, Sandia National Laboratories, Thermal Wave Imaging, Inc. and J. Stephen Cargill, an independent consultant. The Sonic IR program ran from March 2002 through May 2003. Program accomplishments are described briefly in this report. The final monthly report for this program is included as well.

Objective

The objective of this program is to demonstrate that the Sonic Infrared (IR) inspection technique can be used reliably to detect a fatigue crack located at the anti-rotation feature on the F100 first stage turbine disk. As the physics of the mechanical energy to thermal energy conversion for this technique is not well understood at this time, an empirical approach is being used to develop the system parameters that will enable a reproducible inspection technique to be developed for the turbine disk inspection. It is the goal of this program to develop the Sonic IR technique into an inspection method that is ready to pass stringent Air Force probability of detection (PoD) test requirements and to be accepted by the inspection community as a reliable nondestructive evaluation method. Towards those ends, the program accomplishments to date are outlined in the Program Accomplishments section below.

Background

Sonic IR inspection is accomplished by injecting high-powered sonic energy (15-40 kHz) into a sample. Ultrasonic welders are commonly used for this purpose. The mechanical energy interacts with defects, such as a crack, and is converted into thermal energy. This thermal energy is detected on the sample surface by an infrared camera.`

Initial research in this area was conducted by Dr. Edward Henneke et. al. in the early 1980s when the technique was referred to as “vibrothermography.” A German group, led by Dr. Gerd Busse, published on the technique in the mid-1990s and Wayne State University (WSU) researchers revived research in the United States and patented a modified version of the technique in the late 1990s. The WSU group referred to the technique as “thermosonics.”

For the specific example of crack-detection, the Sonic IR technique offers many potential advantages over traditional methods such as fluorescent penetrant inspection (FPI) and magnetic particle inspection (MPI). These advantages include cost, speed, portability, and lack of environmental concerns. The current disadvantage of the

technique is that it has not yet matured to the point of being a robust, reliable, production-ready, user-friendly inspection method.

Program Structure

The program is currently structured as a team effort of multiple subcontractors that bring the expertise required to achieve the objectives of the program. The team members are working together to define the operating parameters required for the inspection of the first stage turbine disk. Other items being addressed by the program team include the acceptance of the technique by the OEM producers of turbine disks for the Air Force and the inspection team located at the Oklahoma City Air Logistics Center that will be included in the deployment of the inspection method into the depot level inspections. Team members are also contributing statistical experimental design expertise and hands-on Sonic IR experience.

Program Accomplishments

Program accomplishments were reported in monthly status reports to AFRL. The final monthly status report on this delivery order is contained in Appendix A. Prior accomplishments are summarized here:

- SAIC conducted a literature search to determine the state of the art of the Sonic IR technique. This information has been supplemented and continuously updated throughout the program by attendance at technical conferences, visits to laboratories (including Lawrence Livermore National Laboratory, Wayne State University, and Thermal Wave Imaging), and conversations with experts in the field.

- SAIC identified and subcontracted appropriate individuals and organizations to provide assistance on this program, including Wayne State University, Sandia National Laboratory, Aerospace Structural Integrity, and Thermal Wave Imaging, Inc. Team members met via teleconference monthly and also held periodic technical interchange meetings.

- The team established technical contacts at engine manufacturers, military depots, and government labs. These contacts are necessary to remain current in the field and also to obtain buy-in on the Sonic IR technique for future use on Air Force engine components.

- SAIC personnel visited Branson engineers to discuss the Branson ultrasonic welder used in most Sonic IR applications. The purpose of the meeting and subsequent discussions was to understand how the welder operates and how best to use it in Sonic IR testing.
- The anti-rotation window on the F100 first stage high-pressure turbine disk was identified as the first inspection area to be targeted by this technique. Scrapped

parts were located at Tinker Air Force Base and appropriated for use by the program.

- SAIC conducted a demonstration of Indigo's ThermoSoniX™ system, the only Sonic IR system commercially available at the time. While it could excite some cracks in some parts, mechanical stability was an obvious shortcoming of the system. Such instability would preclude any degree of reproducibility between tests. Indigo has since decided to halt production and sales of this unit.

- Fixturing and coupling were identified as two of the most important issues for reproducible testing with this technique. SAIC took the task of addressing these issues.

- A fixture for the F100 first stage high-pressure turbine disk was designed and built by SAIC. This fixture allows the disk to rest on it and clamps the disk in the borehole. This clamping is achieved with a lathe chuck that is tightened with a calibrated torque wrench. By clamping the disk in this manner, uniform clamping from test to test is achieved.

- A Sonic IR Working Group composed of university, industry, and government researchers, developers and potential users was formed. The first working group meeting was held in Orlando, FL on March 12, 2003 in conjunction with the ASNT Spring Conference.

- Requirements for a developmental Sonic IR system were defined and all except one of the system components were purchased on this program. These components have been integrated and will be used for in-house technique development, with emphasis on repeatability and robustness.

- Vendors were researched in an effort to find one capable of placing fatigue cracks in an anti-rotation window on an engine disk. A vendor was located for this task and will be placed on contract in the follow-on phase of this program.

- Test plans, based on statistical design of experiments (DoE) principles, were developed under subcontract by Floyd Spencer at Sandia National Laboratory. The first phase of testing focused on interface and vibration isolation materials. This testing was completed. The second phase of testing will be conducted in the follow-on program.

- Thermal Wave Imaging, under subcontract, conducted testing on small fatigue-cracked samples to assist in determining camera requirements. Their findings will assist in future development of a deployable inspection technique. A report documenting these studies is contained in Appendix C.

Summary and Future Work

The work completed in the first stage of the program has set the requirements for the experimental work that will be completed in the next stage of the program. Initially, this work will be performed with smaller test samples until the turbine disks with cracks become available. Using the fatigue-cracked disks, the program will then focus on the second phase of the DoE testing, which will provide a rigorous study of the parameters that may affect the inspection process of the disk. Once the interactions of these parameters are better understood, the technique will be optimized for reliable detection of cracks in the anti-rotation feature of the first stage disk.

Appendix A. Monthly Status Report: May 2003

Monthly Status Report

May 2003

Advanced Thermographic Methods – Sonic IR
AFRL Contract F33615-97-D-5271, NTIP Delivery Order 029

Submitted by:
SAIC Ultra Image International

Introduction

The Materials and Manufacturing Directorate of the Air Force Research Laboratory (AFRL) has initiated a Sonic IR program with SAIC Ultra Image International through Universal Technology Corporation. The AFRL point of contact for this program is Tom Moran from the Nondestructive Evaluation Branch. The program will support the Engine Structural Integrity and Engine Rotor Life Extension Programs of the Air Force. The program includes participation by Wayne State University, Sandia National Laboratories, and J. Stephen Cargill, an independent consultant. The initial phase of the Sonic IR program ran through October 2002 and the second phase of the program will extend through June 2003. Program accomplishments for the last month are described in the following sections of this report.

Technical Progress

The Phase I testing of interface and vibration isolation materials was completed last month. These results are compiled and presented in Appendix A of this report. (APPENDIX B of FINAL REPORT) The analysis of these results in ongoing and will be used to downselect interface materials and vibration isolation materials for the next, larger, phase of testing using the design of experiment that is being prepared by Dr. Floyd Spencer of Sandia National Laboratory.

The task performed by Thermal Wave Imaging (TWI) was completed this month and their report is attached as Appendix B. (APPENDIX C of FINAL REPORT) The focus of the task was to determine which IR cameras can be used for this technique. The conclusions of this analysis, plus additional observations from the work completed by TWI, are summarized by Steve Shepard, president of TWI:

“1. If all experimental parameters are held constant, the sonic IR results are highly repeatable.

2. There is a strong signal dependence on the position of the horn with respect to the crack.

3. Acquisition at a higher frame rate would not significantly affect detectability or length measurement accuracy of the cracks.

4. With a 320 x 240 pixel InSb array and a field of view of approximately 5" x 3.5", cracks with lengths ranging from 0.050" to 0.225" were successfully detected and measured using a 2 kW Branson horn at 50% energy setting. The smallest cracks (0.015" and 0.016") were not detectable at these settings.

5. At the settings described above, measurement error for the crack lengths is on the order of 20%.

6. Detectability of small cracks and measurement accuracy of all cracks could be improved by increasing the pixel density in the field of view. This could be accomplished by either using a camera with a larger focal plane, or moving the 320 x 240 camera closer to the target (and reducing the field of view).

7. Detectability and measurement are considerably improved if time domain processing is applied to the data. Simple subtraction of the presonification background image was the least effective processing method. Calculation of the time derivative of each pixel over a 5-frame duration immediately prior to the end of the sonification period was used to remove extraneous background features and highlight cracks. However, similar results could be obtained by dividing the image acquired just before the end of the sonification period by the presonified image.

8. A proprietary method, Thermographic Signal Reconstruction was effective in distinguishing the actual crack from the blooming that surrounds the crack site. The TSR method was also effective in retrieving weak crack signals that occurred as the input energy was reduced.

9. The large spatial and temporal noise content of data from an uncooled microbolometer camera made it ineffective for application to the crack detection task. Under conditions identical to those described in item 4, above, only the largest crack in the sample set could be reliably detected after signal processing was applied."

Thus, the conclusion of this work is that the high frame rate cameras may not be a requirement for a production-based inspection system, but that uncooled IR cameras do not have sufficient resolution to be used for this application at this time. The evaluation work completed by TWI was performed using the Goodrich PoD test samples that were made available for this program.

Using the list of available fatigue-cracked PoD sample sets supplied by Steve Cargill, the team has chosen the elongated scallop samples for interim testing. This testing will be conducted while waiting for the fatigue cracks to be generated in the engine disks in the next phase of this program. This additional testing will also include some flat plate fatigue cracked samples.

A Polytec PI laser vibrometer was purchased and should be received within the next 2 weeks. A vibrometer owned by San Diego State University will be used until the new one arrives.

SAIC will present a program overview, including details on the design of experiments test matrix, at the Aeromat conference in Dayton, OH, next month. The presentation is co-authored by Dr. Floyd Spencer.

Administrative

The current phase of the Sonic IR program, funded on NTIP Delivery Order 29, will be closed as of the end of this month. Work will continue on this effort using a new contract, on Delivery Order 44, which will be used for this program through the end of August 2003. NTIP II, the next generation IDIQ contract, is expected to begin during that time and future Sonic IR work will continue on that contract.

Financials

Deleted

APPENDIX B. Test Report: Part I – Test Procedure and Results of Phase I Design of Experiments Testing for the Sonic IR Technique

Test dates: March-April 2003
Written by: D. J. Mayton, SAIC
Data collected by: Cody Engstrand, San Diego State University
Experimental design by: Floyd Spencer, Sandia National Laboratories

1.0 Introduction

The work presented in this report is a continuation of testing that was reported previously ("Preliminary Testing of Surface Protection and Vibration Isolation Materials for the Sonic IR Technique"). A series of tests was outlined by Floyd Spencer at Sandia and data were collected at San Diego State University by Cody Engstrand, a graduate student. The results are presented here and analysis of these results is ongoing and will be presented in a subsequent report.

2.0 Experimental Design

The overall experimental design is presented in two phases. The initial phase, discussed here, addresses issues of surface protection materials (SPM) and vibration isolation materials (VIM) and draws upon preliminary testing that was completed earlier in this program using a variety of materials. The second phase will integrate findings from the first phase into a larger experiment that incorporates configuration variations of the Branson welder unit as it is imparting energy into the test specimen.

For the Phase I testing, the laser vibrometer was set up to measure velocity data of the test piece. (Note that in earlier testing displacement data were used.) The vibrometer data are captured and analyzed 5 times for each of the combinations of factors outlined in the test matrix. It should be noted that the ultimate efficacy of the Sonic IR technique is not measured by the vibrometer signal, but rather from whether or not a flaw would be adequately imaged by an IR camera. In the second phase of the experiment, data will be collected from the imaging system as the ultimate evaluation of the performance of the inspection process and the vibrometer data will be obtained as a secondary evaluation factor. Correlations of the two could possibly alter the choice of SPM and VIM provided better criteria for the evaluation of the waveform from the vibrometer is established.

Surface protection and vibration isolation materials need to possess necessary transmission and isolation properties and, for a field inspection environment, they need to be durable. It is likely that durability of the surface protection material will depend upon the tip shape and force applied by the welding horn. For this reason, these factors were included in this initial phase of the experiment. Table B1 shows the factors and levels tested.

Table B1. Initial Factors and Levels.

Factor	Levels
Horn tip	2 – round, flat
Trigger force	2 – 20 lbs, 230 lbs
Surface Protection Material (SPM)	5 – Teflon, PFA, Nomex, Paper (Card Stock), Leather
Vibration Isolation Material (VIM)	3 – Cork, Dynamat, Rubberized cork

Two vibration isolation materials not covered in the previously reported testing are included here. Dynamat, manufactured by Dynamat Control, is an engineered sound control material used in automobiles to reduce road noise and to improve sound system quality. Interim testing showed it to be a promising candidate material and it was added to the test matrix. This was also the case with the rubberized cork material, purchased from McMaster-Carr, Stock Number 9607 K63. It was found to be more durable than plain cork but still possess some desirable properties. All other materials used are described in the earlier report.

3.0 Experimental Setup

A Branson ultrasonic welder (Model 900 ma power supply, Model 921 AES actuator) and an Ometron laser vibrometer (Model VS 100) were used for this testing. The vibrometer data were collected with a National Instruments PCI-6052E multifunction I/O board and the data acquisition was controlled via a National Instruments LabVIEW program. For each test, 50,000 data points were collected at 200 kHz. The test piece used for these tests was a 3.5” diameter, 4.1” tall cylinder of mild steel. It was positioned on the base of the welder unit with the horn contacting it in the center.

A photograph of the welder and vibrometer is shown in Figure B1. The photograph does not include the data acquisition computer.

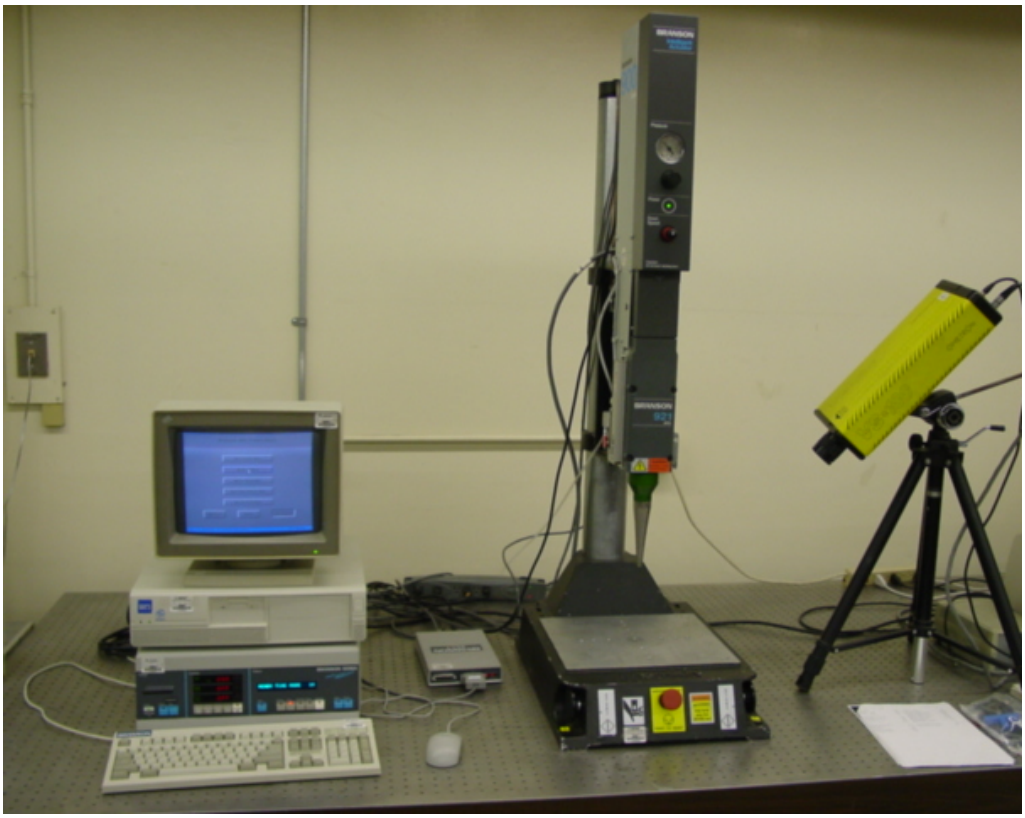

Figure B1. Sonic IR setup for vibration data acquisition.

The Branson welder unit was configured in the “Time” mode. The “Weld Time” was set to 200 ms, the air pressure was set at 36 psi, and the down speed parameter was 1.5. The effect of varying some of these factors will be tested as part of the Phase II test matrix. The energy and power levels varied for each test.

Since it is not yet known which frequency or frequency range produces the best Sonic IR signal, the AC rms average of the velocity data was calculated. (This data could be re-analyzed in the future if a particular frequency or range is determined to be most relevant for Sonic IR testing of the engine disks.)

4.0 Results

The digitized laser vibrometer velocity data were analyzed by calculating the AC (alternating current) rms (root mean square) average for each 250 ms waveform. This AC rms average gives a quantitative measure of vibration and can be used to compare the behavior of the different combinations of factors. It was not possible to collect data for some of the combinations of factors since the welder unit locked up and gave an error prior to the completion of the 200 ms weld cycle.

The results of the Phase I testing are listed in Table B2. For each combination of factors, 5 data sets were collected and the AC rms value calculated. Data is listed in the following format:

(A)
(B)
(C)

where

A = average of 5 data sets
B = highest value
C = lowest value.

Cases in which the welder gave an error and data were not available are noted by “na”. This data will be analyzed for trends and will be summarized in a subsequent progress report.

Table B2. Phase I Test Results.

Horn Tip		Flat														
VIM		Cork					Dynamat					Rubberized Cork				
SPM		Pap	Tef	PFA	Nom	Lea	Pap	Tef	PFA	Nom	Lea	Pap	Tef	PFA	Nom	Lea
Horn Trigger Force (lbs)																
20		**1.190** (1.69) (1.04)	**1.154** (1.21) (1.11)	**1.062** (1.15) (1.01)	**1.004** (1.25) (0.83)	**0.262** (0.31) (0.20)	**1.093** (1.12) (1.07)	**1.179** (1.22) (1.14)	**1.062** (1.09) (1.04)	**0.992** (1.09) (0.85)	**0.285** (0.31) (0.24)	**0.936** (0.96) (0.89)	**1.008** (1.05) (0.96)	**0.902** (0.92) (0.89)	**1.031** (1.20) (0.89)	**0.355** (0.39) (0.28)
230		**3.230** (3.31) (3.11)	na	na	**3.386** (3.62) (3.30)	**2.332** (2.37) (2.28)	na	na	na	**3.672** (4.29) (3.10)	**2.195** (2.42) (1.76)	**3.509** (3.74) (3.25)	na	na	**3.701** (4.11) (3.37)	**2.373** (2.58) (2.17)

Horn Tip		Round														
VIM		Cork					Dynamat					Rubberized Cork				
SPM		Pap	Tef	PFA	Nom	Lea	Pap	Tef	PFA	Nom	Lea	Pap	Tef	PFA	Nom	Lea
Horn Trigger Force (lbs)																
20		**1.072** (1.10) (1.05)	**1.053** (1.10) (1.02)	**1.061** (1.10) (1.03)	**0.839** (0.88) (0.79)	**0.095** (0.11) (0.08)	**1.184** (1.22) (1.14)	**1.254** (1.29) (1.22)	**1.518** (1.57) (1.48)	**0.933** (0.98) (0.89)	**0.104** (0.14) (0.09)	**0.924** (0.97) (0.87)	**0.969** (1.01) (0.94)	**1.187** (1.22) (1.15)	**0.911** (1.06) (0.86)	**0.098** (0.12) (0.08)
230		**3.804** (3.91) (3.70)	**3.795** (3.83) (3.76)	**3.605** (3.75) (3.47)	**3.605** (3.66) (3.44)	**1.338** (1.56) (1.22)	**2.962** (3.04) (2.86)	**2.050** (2.09) (2.00)	**1.962** (2.10) (1.86)	**2.833** (3.08) (2.43)	**1.349** (1.49) (1.23)	**3.848** (3.91) (3.76)	**3.874** (3.94) (3.82)	**3.744** (3.80) (3.65)	**3.614** (3.70) (3.54)	**1.644** (1.80) (1.53)

VIM = Vibration Isolation Material, SPM = Surface Protection Material, Pap = paper (card stock), Tef = Teflon film, Nom = 10 mil Nomex, Lea = leather.

APPENDIX C. SAIC – TWI Sonic IR Final Report

Issues in Sonic IR Crack Detection

Final Report

Prepared by

Thermal Wave Imaging, Inc.

Under subcontract 4400064738, subproject 01-0286-38-2508-000
Science Applications International Corp.

May 16, 2003

Issues in Sonic IR Crack Detection

Introduction

The following report summarizes a study of sonic IR inspection on a set of crack samples intended to be representative of defects in an airborne turbine engine component. The goal of this study was to determine the feasibility of detecting typical cracks using reduced energy methods, augmented by signal processing, as opposed to the brute force excitation / visual detection methods that are currently used. Experiments were conducted to determine whether robust and repeatable detection and measurement of crack defects could be accomplished using a well-defined procedure that was appropriate for low-level inspection personnel. It should be noted that although it was necessary to address a number of issues related to procedures, repeatability, sensitivity and basic phenomenology, this effort is not intended to serve as a substitute for comprehensive study and evaluation of these issues.

Experimental Set-up

The samples were evaluated using the EchoTherm VT vibrothermographic inspection unit, which employs a 2 kW ultrasonic horn for excitation and an Indigo Merlin Mid IR camera (60 Hz frame rate, 320 x 256 InSb focal plane array) for detection. Data was acquired and analyzed using the EchoTherm VT software.

In order to compare results over a set of samples, it was first necessary to minimize variability in the positioning, excitation, clamping and imaging of the samples. A small Delrin jig was constructed to hold the part in firmly place without excessive damping. Although there were small variations in the size of the sample plates, a single jig setting could be used to hold all samples in exactly the same position relative to the horn and camera.

Several decisions were made regarding experimental parameters in the interest of consistency. However, other concurrent studies may suggest different, and possibly better answers. The particular issues are described below:

Horn placement: The relatively small size of the sample made it difficult to place the horn on the face of the sample without at least partially blocking the camera line of sight. Furthermore, direct placement on the sample face increased the risk of damage to the sample. Instead, the sample was excited on its edge.

Horn coupling: Direct metal to metal contact between the sample and Ti horn caused damage to the sample surface, and often yielded inconsistent results. Various coupling media were evaluated, including Al sheet plates and foil and copper. Although each of these alternatives produced positive results, there was considerable shot-to-shot variation that depended on the details of the coupling medium geometry and precise placement. In order to insure optimum repeatability, the horn tip was wrapped with Teflon tape before each shot (shot to shot repeatability is quite high with a new piece of Teflon for each shot, but it falls off rapidly if a single piece is used repeatedly).

Energy parameters: In all experiments, sonic energy at 15 kHz was applied for a duration of 0.5 seconds. Although it is possible to use either shorter or longer energy bursts, there is no significant increase in detectability with a longer burst. However, a 0.5 second burst provides sufficient data for oversampling using a 60 Hz frame rate camera, so that time history based signal processing methods can be applied.

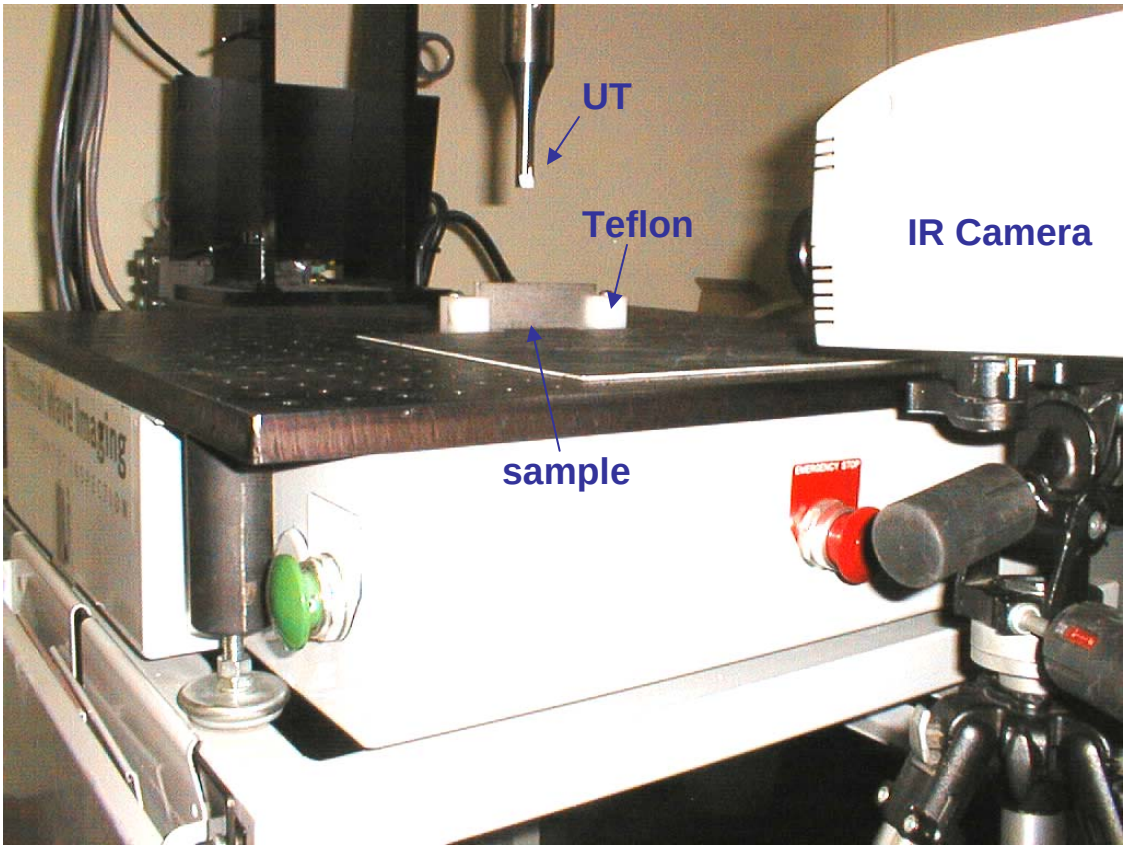

Figure C1: Experimental setup for crack sample evaluation.

In addition to the Merlin camera, preliminary experiments were conducted with cameras including an uncooled microbolometer (FLIR Thermovision), a Quantum Well (QWIP) focal plane array (FLIR SC-3000), and a high speed InSb focal plane array (Indigo Phoenix). Results from the Merlin, Phoenix and QWIP were quite similar. The Phoenix offers high frame rate capability, however there was no detectability improvement at high speed. The QWIP operates at a longer wavelength (8-9 um) but there was no particular advantage gained for crack detection in the present sample set. However, the results from the uncooled camera were substantially worse than the others. Instability of the signal over the sonic excitation time and significant fixed pattern spatial noise limited the degree of improvement that cold be achieved through signal processing. Based on these considerations, the bulk of the experiments were conducted with the Merlin camera.

Surface Preparation

No surface preparation was applied to the samples. However, Teflon tape was used as a coupling layer between the horn and sample.

Repeatability

Repeatability of both image and temporal inspection results was evaluated. Ten (10) identical sequences of a sample with 2 cracks (19B, with crack lengths 0.050” and 0.098”) were acquired, and the process was repeated at 4 different input energy levels (20, 30, 40 and 50% energy). In the image at the peak contrast time, both the amplitude and the time derivative along the length of the crack were recorded. The temperature-time evolution of the temperature at the center of the crack was also recorded. In these experiments, there was no movement of the sample or change in the horn position between shots, so that shot-to-shot conditions were essentially identical. Acquisitions were performed at approximately 20 second intervals.

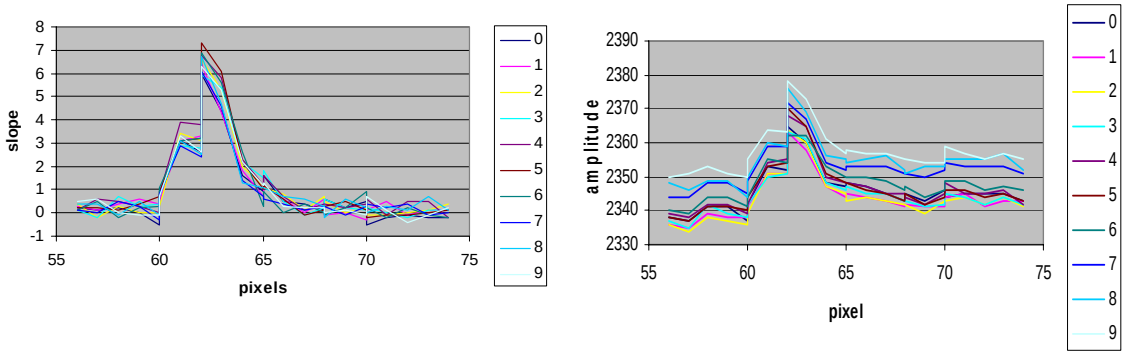

Figure C2: Repeatability results for a 0.098” crack (19B, crack 2). Left: Slope along the crack at the peak contrast time. Right: Amplitude along the crack at the peak contrast time.

The results in shown in figure C2 show typical performance. The slope and amplitude results are quite similar, and both exhibit a high degree of shot to shot repeatability. However, the amplitude results show a gradual increase in offset over time, due to bulk heating of the sample, either through a frictional mechanism or contact with the horn and jig surfaces. This offset does not pose a significant problem. However, the slope signal is near zero away from the crack, while the amplitude signal displays a floating background signal that complicates measurement of the precise crack boundaries.

Examination of temperature time evolution for the same crack (Fig. C3) also shows a high degree of repeatability (except for a dc offset) over 10 consecutive acquisitions. They essential features of the time evolution appear in each trace, including the peak and a sudden dip in crack amplitude in the larger (0.098”) crack.

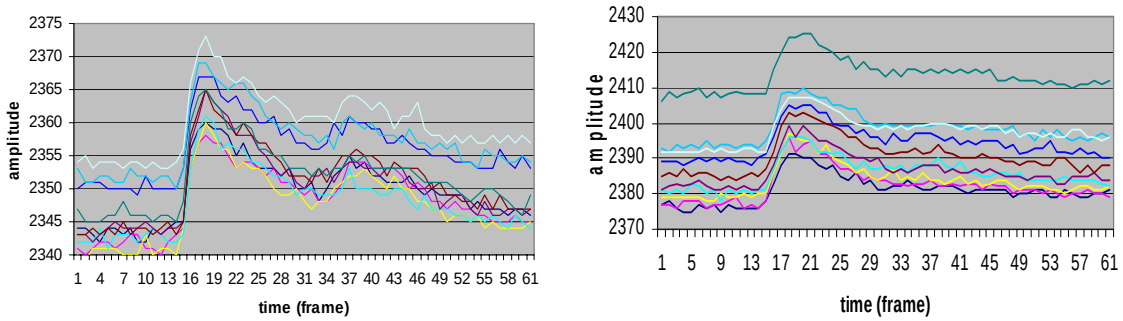

Figure C3. Time evolution of crack center for cracks in sample 19B. Left: Crack 2 (L=0.098”). Right: Crack 1 (L=0.050”).

Horn Proximity to Crack

Signal repeatability as a function of the proximity of the horn to the crack location was tested by performing the 10 shot repeatability test once, and then again after rotating the sample by 180 degrees. The horn was placed approximately 1/3 of the sample length from the left edge of the sample, so that the contact point would be near and then far from each crack site in the two orientations. Although results at each orientation are quite repeatable, comparison of near and far orientation results for a given crack raise questions that are beyond the scope of this investigation (Fig.C4)

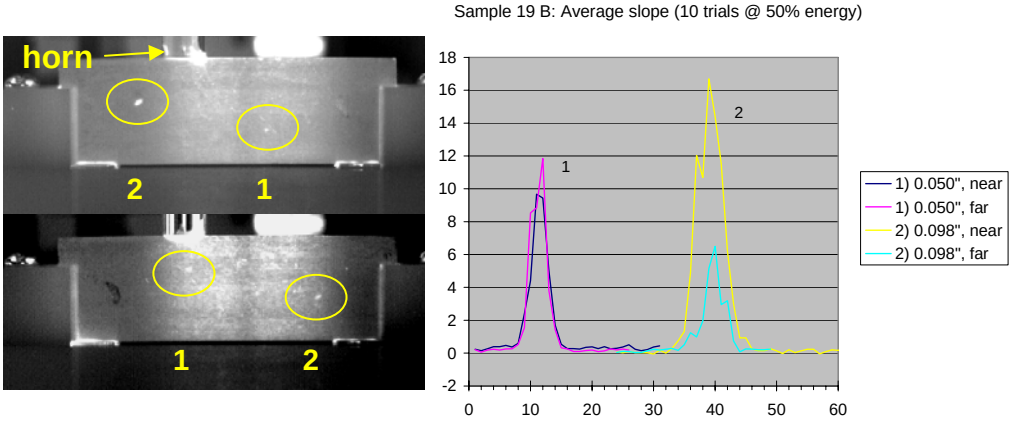

Figure C4: Left: Sample 19 B at 2 orientations with respect to the sonic horn. Right: Slope curves along the cracks. Slope results from 10 consecutive trials have been averaged to create noise reduced curves for comparison.

In the data shown in Figure C4, agreement between the near and far orientation data is quite good for the smaller (0.050”) crack. However, slope amplitude for the larger crack are extremely different at the different orientations, although the overall shape is preserved. This data is inconclusive, but suggests that there are phenomenological issues associated with sample geometry and insertion point that are beyond the scope of this investigation. However, it is worth noting that if all conditions are held constant, repeatability is preserved regardless of the location of the insertion point.

Crack Length Measurement

Crack lengths were measured using the slope image measured over the 5 frame interval immediately preceeding (and including) the peak contrast time. During this interval, the signal is generally increasing monotonically, although noise affects the profile significantly in some cases. A line cursor is manually placed on the image of the crack in the analysis software, and profile of the curve is analyzed. To minimize noise contributions, three point nearest neighbor smoothing is performed on the line profile, and the Full Width, Half Maximum (FWHM) value of the crack profile is calculated. Results from the length measurement of the sample set at 50% energy are shown in Figure C5.

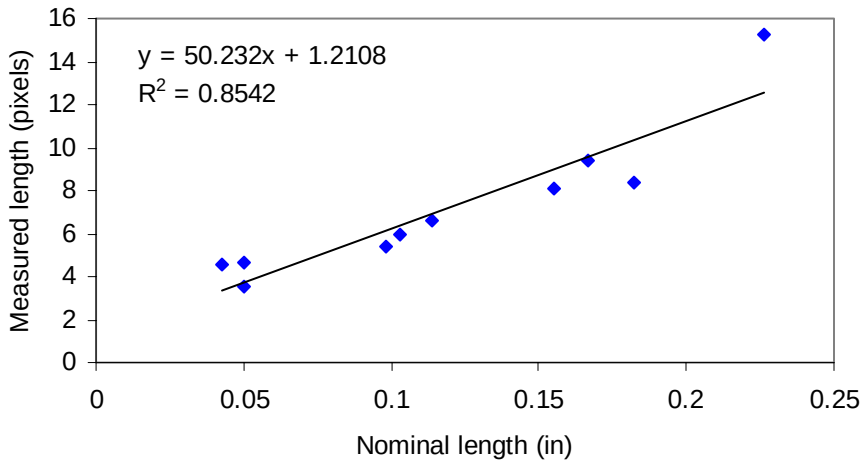

Figure C5: Crack length measurement at 50% input energy.

General agreement between nominal and measured crack length values is good. However, there are several issues worth noting:

1. The FWHM of the slope was used to measure length so that a consistent metric could be applied without arbitrary decisions on placement of endpoints.
2. The smallest cracks in the sample set (9A and 13 B, at L = 0.015” and 0.016”, respectively) were not detectable, and were not included in the measurement results.
3. The accuracy of these measurements is limited in part by the resolution of the camera. The smallest detectable cracks (0.046” and 0.050”) span lengths of only a few pixels. Although fractional pixels lengths are used to calculate crack size, accuracy of the measurement is compromised when the crack length is on the order of the pixel size. In the configuration used for these measurements, there are approximately 72.26 pixels per inch, so that a 0.050” crack spans 3-4 pixels, and the span of the smallest cracks in the set (~0.015”) is a single pixel. The situation can be improved by either moving the camera closer to the sample (at the risk of possible damage to the camera optics by flying debris) or using

specialty optics. In either case, one sacrifices the wide field of view capability. Another alternative which does not necessarily sacrifice large area capability is to use a large format focal plane array camera. However, at present the cost of these cameras is significantly higher than 320 x 240 pixel models.

Image Visualization

With the exception of the smallest cracks in the sample set (~0.015”), all of the cracks were successfully detected by an operator without reference to the documentation provided. However, in some cases visual detection in the raw images at the peak contrast time was not successful, due to the presence of extraneous features in the image, nonuniform temperature distribution across the sample, and the relatively large signal from the horn at the insertion point. False calls, based on surface features, could also occur using raw image visualization, as shown in Figure C6.

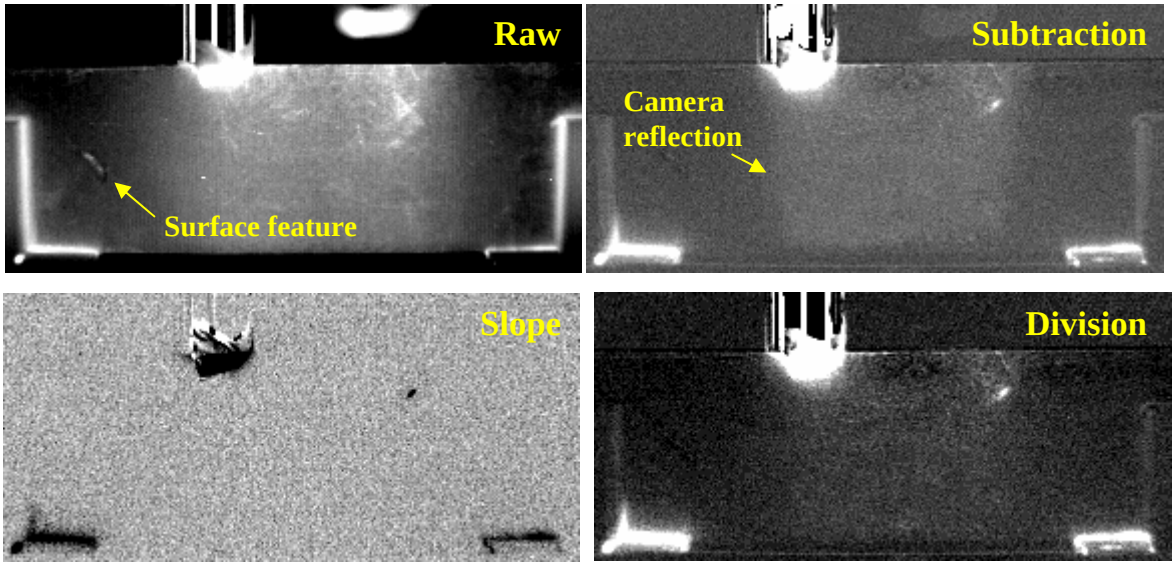

Figure C6: Processing alternatives are shown for a 0.182” long crack (Sample 22A). In the raw image (upper left), the actual crack is obscured by surface scratches, and a benign surface feature appears to be a crack. Various degrees of improvement are possible using subtraction, division or slope methods.

Improved crack visualization was accomplished using subtraction, division and slope processing methods. A proprietary method, Thermographic Signal Reconstruction (TSR), was also evaluated. In the subtraction method, an image acquired immediately before sonic energy is applied and subtracted from the image acquired at the peak contrast time. The degree of subtraction may be varied, since direct subtraction may result in image artifacts. The division uses the same pre-sonification image to divide the peak contrast image. However, the slope image generated over the frames immediately preceeding the peak contrast image offers the more complete removal of background features and effective image segmentation than subtraction or division.

The TSR method is based on creating separate functional representations of the heating and cooling segments of the time evolution of each pixel. The primary advantage of this approach is that it allows visualization of instantaneous time derivatives that are generally more accurate and less susceptible to temporal noise than comparable slope images generated by fitting a straight line over data from a few consecutive frames. TSR also supports creation of a 2nd derivative image. Typical TSR results are shown in Fig. C7.

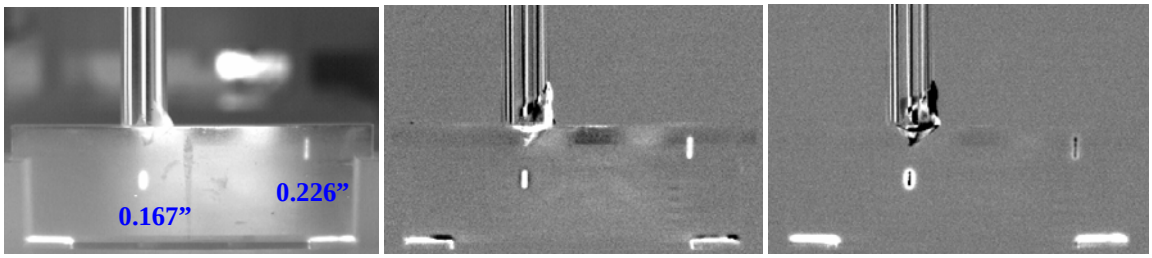

Figure C7: (Left to right) Raw, and 1st and 2nd derivative images of Sample 28B.

The result shown on Figure C7 illustrates a useful aspect of the reconstructed second derivative crack images. Although the 2 crack indications are clearly visible in the raw and reconstructed image, there is considerable thermal blooming in the vicinity of the crack. However, in the TSR second derivative, a dark image of the actual crack is seen within the larger image.

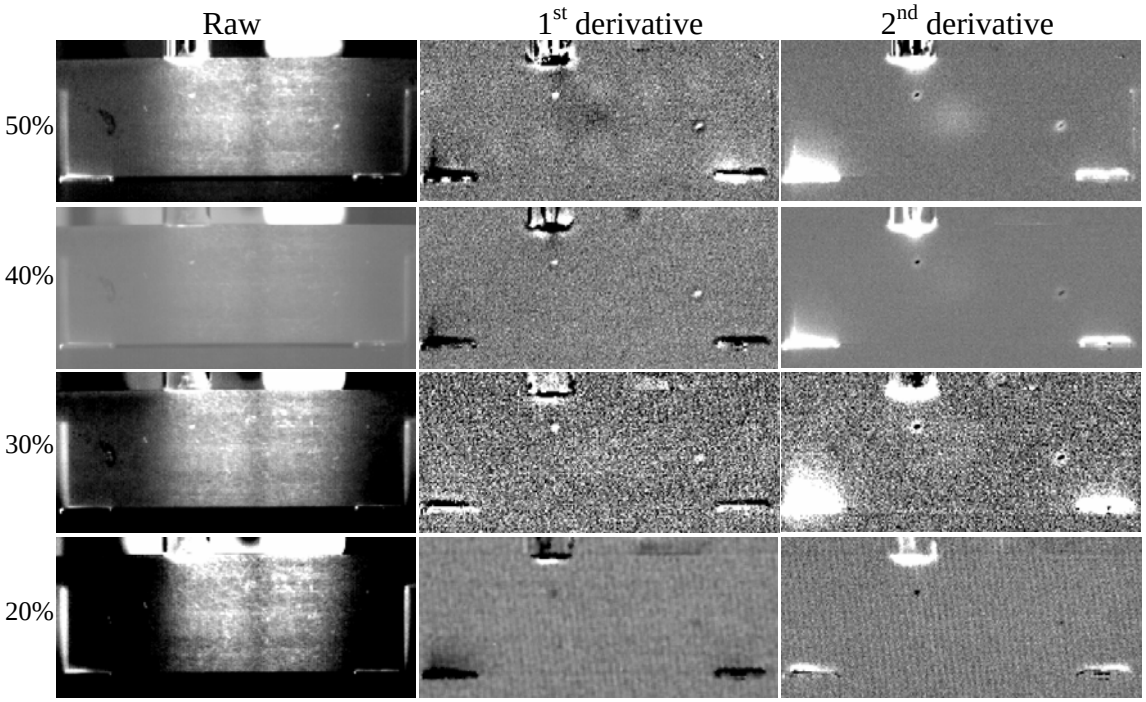

Figure C8: Raw and reconstructed derivative images of Sample 19 B (crack sizes 0.050” and 0.098”) at various input energy levels. At lower levels, the cracks are not detectable in the raw images, but they do appear in the reconstructed derivative images.

The reconstructed data is particularly useful as input energy is decreased (Figure C8), and visualization of cracks in the raw image becomes complicated, and in some cases impossible.

Discussion and Recommendations

This study was based on analysis of a small numbers of sample coupons intended to mimic the acoustic response of a large turbine component. Inspection of the actual component will require careful analysis of the geometry and acoustic response of the part. Furthermore, the part is quite massive, compared to the small sample coupons, so that energy input requirements and signal levels may be significantly different than those reported here. Issues related to analysis of the actual component are beyond the scope of this study. However, to the extent that the sample coupons provided represent the response of the actual sample, we offer the following recommendations and guidelines for implementation.

In the experiments we conducted, all cracks with lengths of 0.050” or greater were successfully detected. Smaller cracks, with lengths of 0.015” and 0.016” were not detected. These results were achieved using a 2 kW ultrasonic horn at 50% energy setting, an InSb focal plane array camera with a 320 x 240 pixels operating at 60 Hz. The field of view of the camera in the plane of the sample was approximately 4.625” x 3.5”. There are several ways to improve detection capability for small cracks, in order to reduce the minimum detectable defect size. Increasing energy input, improving coupling, optimizing clamping and horn pressure, and optimal horn placement are all factors than can improve signal output. However, for the range of signal levels encountered in this study, detection of small cracks would be improved by either configuring the optics to allow a closer working distance (thus reducing the field of view), or using a camera with a higher pixel density (more expensive). The smallest cracks in the sample group span only 1-3 pixels under the configuration employed in this study. As a result, it is difficult to discriminate features on that scale from the combined effects of spatial and temporal noise. Either of the suggested improvements will results in more pixels on a crack, increasing the likelihood of detection.

If the goal of the proposed inspection is precise measurement of crack lengths, the importance of increased pixel density is considerably greater. Given that measurement of an arbitrarily oriented crack involves interpolation, and calculation of fractional pixel values, there is a significant penalty in terms of measurement accuracy when only a small number of pixels span the crack. The problem is compounded in the typical case where the orientation of the crack is not perfectly aligned with the rows and columns of the focal plane. In such cases, a crack that is a perfect straight line is imaged as a jagged line, reducing measurement accuracy. Both of these problems subside in inverse proportion to the pixel density.

In terms of currently available technology, the next largest commercially available camera array size is approximately 640 x 480 pixels. If a similar experimental configuration were used, the field of view would be unchanged, but the density of pixels would be quadrupled, resulting in a significant improvement in measurement accuracy. Although detectability of small defects would also occur, and it should be possible to detect the 0.015” scale cracks.

Based on this study, we conclude that the density of pixels in the field of view is a more important consideration than the frame rate of the camera. Although high frame rate

imaging is useful for studying the phenomenology of heat generation, it did not prove to be necessary for detection of the cracks in the sample set. In the numerous trials performed on these samples under various conditions, we did not encounter a situation where a sample (other than the 2 smallest cracks) did not produce a detectable signal that persisted for the duration of several frame periods at 60 Hz.

In the early stages of this study, cameras based on different detector technologies were evaluated. Due to logistic and schedule considerations, the bulk of experimentation was performed using an InSb camera. However, we found that nearly identical performance could be obtained using a camera based on a quantum well (QWIP) focal plane. We also evaluated a low cost microbolometer camera. However, we found that both the spatial and temporal noise were significantly higher than that in either the QWIP or InSb camera, and as a result, only the largest crack in the sample set could be detected after signal processing.

In analyzing the experimental data, it was possible to significantly improve both detectability and measurement performance though some degree of signal processing. We found that subtraction, the most commonly used processing approach, was also the least effective. Results using either slope or division methods were more successful in isolating crack features, and providing more consistent measurement results. We found the slope approach best of these three methods for use in length measurement, as the slope signal is consistently relatively flat with mean zero in non-crack regions.

The Thermographic Signal Reconstruction (TSR) method was also evaluated. For large cracks, it offers the advantage of distinguishing the actual crack from thermal blooming that occurs as heat flows away from the crack site. The TSR approach also offered the best detectability performance in weak signal situations, as the input energy was decreased.